

Can User-Level Probing Detect and Diagnose Common Home-WLAN Pathologies?

Partha Kanuparth^{†,*}, Constantine Dovrolis[†], Konstantina Papagiannaki[‡],
Srinivasan Seshan[§], Peter Steenkiste[§]

[†] Georgia Institute of Technology [‡] Telefonica Research [§] Carnegie Mellon University

Abstract

Common Wireless LAN (WLAN) pathologies include low signal-to-noise ratio, congestion, hidden terminals or interference from non-802.11 devices and phenomena. Prior work has focused on the detection and diagnosis of such problems using layer-2 information from 802.11 devices and special-purpose access points and monitors, which may not be generally available. Here, we investigate a user-level approach: is it possible to detect and diagnose 802.11 pathologies with strictly user-level active probing, without any cooperation from, and without any visibility in, layer-2 devices? In this paper, we present preliminary but promising results indicating that such diagnostics are feasible.

1 Introduction

Most home networks today use an 802.11 Wireless LAN (WLAN) with a single Access Point (AP), typically operating in Distributed Coordination Function (DCF) mode. Home WLANs often suffer from various performance pathologies, such as low signal strength, significant noise, interference from external non-802.11 devices and physical phenomena, various forms of fading, hidden terminals from devices in the same WLAN or in nearby WLANs, or congestion. These pathologies can result in throughput degradation, significant jitter and packet losses. To make things worse, due to the wireless nature of the medium, troubleshooting WLAN performance is hard even for experts, leave alone home users.

User-level probing is a well-established research area in wired networks and it is used in practice to infer various properties and problems in such networks. In the wireless domain, on the other hand, it is still unclear whether user-level probing can be nearly as effective. A main motivation behind this work is to answer the following “intellectual curiosity” question: *is it possible to*

diagnose common WLAN performance problems using active probing, without any information from, or modifications to, the 802.11 devices or AP? The methods presented in this paper show promising (but preliminary) results, potentially opening a new research thread within the area of wireless networks.

Specifically, our objective is to construct a user-level tool for any 802.11 DCF WLAN that can detect: a) low Signal-to-Noise Ratio (SNR), b) Hidden Terminals (HT), or c) congestion. The methodology we propose, referred to as *WLAN-probe*, is a simple, easy-to-use, client-server application that eliminates the need for vendor-specific network card (NIC), driver, AP, monitoring devices, or network modifications. It is also portable across platforms, since it only requires a user-level socket library (e.g., Berkeley sockets, POSIX, or Winsock APIs).

There are several reasons for a user-level probing tool:

Usability: We want to build a diagnostic tool that would not require the user to install a specific NIC, AP, or modify the kernel (moreover, it would not require administrative privileges). The user would just run a *single instance* of the WLAN-probe client at the wireless link that appears problematic.

Hardware-agnostic: Most wireless cards today export some form of signal strength; for example, the Received Signal Strength Indicator (RSSI). RSSI implementations are vendor-specific and they are not uniform across NICs. A user-level approach avoids the need to calibrate NIC statistics across devices and drivers on different OSes.

Software-agnostic: A user-level approach eliminates the need to write and maintain a hardware-compatibility layer for different OSes that would expose NIC statistics at user-space. An example of that approach is WRAPI [1], designed to work on Windows XP with NICs supporting NDIS 5.1 drivers.

*Contact author: partha@cc.gatech.edu

Passive inference: Understanding active probing in the wireless domain may also enable methods for passive inference. For example, is it possible to troubleshoot client performance at a remote web or video server using strictly application traffic?

State-of-the-art diagnosis tools require (or modify) vendor-specific drivers and NICs, or they require special monitors at the home network; we cover these approaches in the related work section.

WLAN-probe is based on two fundamental effects: a) the fact that low-SNR and HTs cause a dependency between packet size and retransmission probability, while congestion does not do so, and b) the fact that low-SNR conditions differ significantly from HTs in the delay or loss temporal correlations they create. However, measuring layer-2 retransmissions and delays is not feasible without information from the link layer. In this short paper, we present the basic ideas and algorithms for user-level inference of link layer effects, with a limited testbed evaluation. In future work, we will conduct a more extensive evaluation, experiment with actual deployment at several home networks, and expand the set of diagnosed pathologies.

We consider the following architecture, which is typical for most home WLANs (see Figure 1). A single 802.11 AP is used to interconnect a number of wireless devices; we do not make any assumptions about the exact type of the 802.11 devices or AP. We assume that another computer, used as our WLAN-probe measurement server S is connected to the AP through an Ethernet connection. This is not difficult in practice given that most APs provide an Ethernet port, as long as the user has at least two computers at home. The key requirement for the server S and its connection to the WLAN AP is that it should not introduce significant jitter (say more than 1-3msec). The server S allows us to probe the WLAN channel without demanding *ping-like* replies from the AP and without distorting the forward-path measurements with reverse-path responses. The measurements can be conducted either from C to S or from S to C to allow diagnosis of both channel directions; we focus on the former. Note that some APs or terminals that are not a part of our WLAN may be nearby (e.g., in other home networks) creating hidden terminals and/or interference, while the user has no control over these networks.

We have conducted all experiments in this paper using a testbed that consists of 802.11g Soekris net4826 nodes with mini-PCI interfaces. The mini-PCI interfaces host either an Atheros chipset or an Intel 2915ABG chipset, with the MadWiFi and ipw2200 drivers respectively (on the Linux 2.6.21 kernel). The MadWiFi driver allows us to choose between four rate adaptation modules. We disable the optional MadWiFi features referred to as *fast frames* and *bursting* because they are specific to Mad-

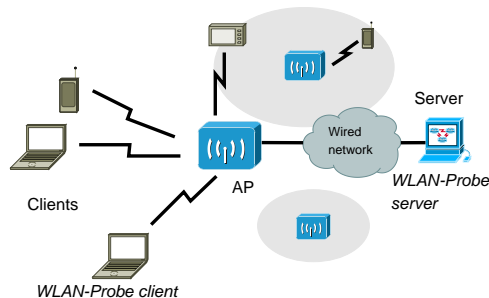


Figure 1: System architecture.

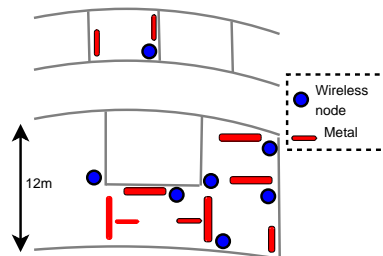


Figure 2: Testbed layout.

WiFi's *Super-G* implementation and they can interfere with the proposed rate inference process. The testbed is housed in the College of Computing at Georgia Tech, and the geography is shown in Figure 2.

Related work

There is significant prior work in the area of WLAN monitoring and diagnosis. However, to the extent of our knowledge, there is no earlier attempt to diagnose WLAN problems using exclusively user-level active probing, without any information from 802.11 devices and other layer-2 monitors. User-level active probing has been used to estimate *conflict graphs* and hidden terminals, assuming that the involved devices cooperate in the detection of hidden terminals [5, 18, 19]. Instead, with WLAN-probe, hidden terminals may not participate in the detection process (and they may be located in different WLANs). Passive measurements have also been used for the construction of conflict graphs [6, 11, 24]. Earlier systems require multiple 802.11 monitoring devices [8, 9, 17], NIC-specific or driver-level support for layer-2 information [7, 23], and network configuration data [4]. Model-based approaches use transmission observations from the NIC to predict interference [14, 16, 21, 22]. Signal processing-based approaches decode PHY signals to identify the type of interference [15]; some commercial spectrum analyzers [2, 3] deploy such monitoring devices at vantage points.

2 Wireless Access Delay

The proposed diagnostics are based on a certain component of a probing packet’s One-Way Delay (OWD), referred to as *wireless access delay* or simply *access delay*. Intuitively, this term captures the following delay components that a packet encounters at an 802.11 link: a) waiting for the channel to become available, b) a (variable) backoff window before its transmission, c) the transmission delay of potential retransmissions, and d) certain constant delays (DIFS, SIFS, transmission of ACKs, etc). The access delay does *not* include the potential queuing delay at the sender due to the transmission of earlier packets, as well as the latency for the first transmission of the packet. The access delay captures important properties of the link layer delays which allow us to distinguish between pathologies; further, we can estimate it with user-level measurements.

Before we define the wireless access delay more precisely, let us group the various components of the OWD d_i of a packet i from C to S (see Figure 1) into four delay components. We assume that the link between the AP and S does not cause queuing delays. First, packet i may have to *wait* at the sender NIC’s transmission queue for the successful transmission of packet $i - 1$ - this is due to the FCFS nature of that queue and it does not depend on the 802.11 protocol. If the time-distance (“gap”) between the arrival of the two packets at the sender’s queue is g_i , packet i will have to wait for w_i before it is available for transmission at the head of that queue, where:

$$w_i = \max \{d_{i-1} - g_i, 0\} \quad (1)$$

We can estimate w_i only if packet $i - 1$ has *not* been lost - otherwise we cannot estimate the access delay for packet i . The second delay component is the *first* (and potentially last) *transmission delay* of packet i . In 802.11, packets may be retransmitted several times and each transmission can be at a different layer-2 rate in general. The ratio $s_i/r_{i,1}$ represents the first transmission’s delay, where s_i is the size of the packet (including the 802.11 header and the frame-check sequence) and $r_{i,1}$ is the layer-2 rate of the first transmission; we focus on the estimation of $r_{i,1}$ in the next section. The third delay component c includes various *constant latencies* during the first transmission of a packet; without going into the details (which are available in longer descriptions of the 802.11 standard), these latencies include various DIFS/SIFS segments and the layer-2 ACK transmission delay (which is always at the same rate). Finally, there is a *variable delay* component β_i . When the packet is transmitted only once, β_i consists of the waiting time (“busy-wait”) for the 802.11 channel to become available as well as a random backoff window (uniformly distributed in a certain number of time *slots*). If the packet has to be

transmitted more than once, β_i also includes *all the additional delays* because of subsequent retransmission latencies, busy-wait, backoff times and constant latencies. These delay components are illustrated in Figure 4. We define the wireless access delay a_i as

$$a_i = c + \beta_i \quad (2)$$

and so it can be estimated from the OWD as

$$a_i = d_i - w_i - \frac{s_i}{r_{i,1}} \quad (3)$$

where w_i is derived from Equation 1.

Another way to think about the wireless access delay is as follows. Suppose that we compare the OWD of a packet that traverses an 802.11 link with the OWD of an equal-sized packet that goes through a work-conserving FCFS queue with constant service rate r (e.g., a DSL or a switched Ethernet port). The OWD of the latter would include the sender waiting time w_i and the transmission latency s_i/r . In that case the term a_i would only consist of the queuing delay due to cross traffic that arrived at the link before packet i . In the case of 802.11, the link is *not* work-conserving (packets may need to wait even if the channel is available), the transmission rate can change across packets, and there may be retransmissions of the same packet. Thus, the wireless access delay captures not only the delays due to cross traffic, but also all the additional delays due to the idiosyncrasies of the wireless channel and the 802.11 protocol. A significant increase in the access delay of a packet implies either long busy-waiting times due to cross traffic, or problematic wireless channel conditions due to low SNR, interference etc. In the following sections we examine the information that can be extracted from either temporal correlations in the access delay, or from the dependencies between access delay and packet size. It should be noted that the *access delay* can have additional applications in other wireless network inference problems (such as available bandwidth estimation), which we plan to investigate in future work.

Diagnosis tree and probing structure

Having defined the key metric in the proposed method, we now present an overview of the WLAN-probe diagnosis tree that allows us to distinguish between pathologies (see Figure 3). We start by analyzing each packet train separately, and use a novel dispersion-based method to infer the per-packet layer-2 transmission rate, when possible (Section 3). Based on the inferred rates, we can estimate the wireless access delay for each packet. We then examine whether the access delays increase with the packet size (Section 4). When this is *not* the case, the WLAN pathology is diagnosed as congestion. On

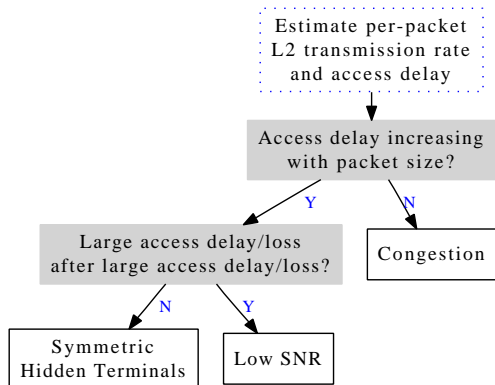


Figure 3: WLAN-probe decision tree.

the other hand, when the access delays increase with the packet size, the observed pathology is due to low SNR or hidden terminals. We distinguish between these two pathologies based on temporal correlation properties of packets that either encountered very large access delays or that were lost at layer-3 (Section 5).

To conduct the previous diagnosis tests, we need to probe the WLAN channel with multiple packet trains and with packets of different sizes. Each train provides a unique “sample” - we need multiple samples to make any statistical inference. Each train consists of several back-to-back packets of different sizes. The packets have to be transmitted back-to-back so that we can use dispersion-based rate inference methods, and they have to be of different sizes so that we can examine the presence of an increasing trend between access delay and size. Specifically, the probing phase consists of 100 back-to-back UDP packet trains. These packet trains are sent from the WLAN-probe client C to the WLAN-probe server S . The packets are timestamped at C and S so that we can measure their *relative* One-Way Delay (OWD) variations. The two hosts do not need to have synchronized clocks, and we compensate for clock skew during each train by subtracting the minimum OWD in that train. The send/receive timestamps are obtained at user-level. There is an idle time of one second between successive packet trains. Each train consists of 50 packets of different sizes. About 10% of the packets, randomly chosen, are of the minimum-possible size (8-bytes for a sequence number and a send-timestamp, together with the UDP/IP headers) and they are referred to as *tiny-probes* - they play a special role in transmission rate inference (see Section 3). The size of the remaining packets is uniformly selected from the set of values $\{8 + 200 \times k, k = 1 \dots 7\}$ bytes.

3 Transmission Rate Inference

The computation of the wireless access delay requires the estimation of the rate $r_{i,1}$ for the *first transmission* of each probing packet. Even though capacity estimation using packet-pair dispersion techniques in wired networks has been studied extensively [10, 13], the accuracy of those methods in the wireless context has been repeatedly questioned [20]. There are three reasons that capacity estimation is much harder in the wireless context and in 802.11 WLANs in particular. First, different packets can be transmitted at different rates (i.e., time-varying capacity). Second, the channel is not work-conserving, i.e., there may be idle times even though one or more terminals have packets to send. Third, potential layer-2 retransmissions increase the *dispersion* between packet pairs, leading to underestimation errors. On the other hand, there are two positive factors in the problem of 802.11 transmission rate inference. First, there are only few standardized transmission rates, and so instead of estimating an arbitrary value we can select one out eight possible rates. Second, most (but not all) 802.11 rate adaptation modules show strong temporal correlations in the transmission rate of back-to-back packets. In the following, we propose a transmission rate inference method for 802.11 WLANs. Even though the basic idea of the method is based on packet-pair probing, the method is novel because it addresses the previous three challenges, exploiting these two positive factors.

Approach: Recall that WLAN-probe sends many packet trains from C to S , and each train consists of 50 back-to-back probing packets (i.e., 49 packet-pairs). Consider the packets $i-1$ and i for a certain train; we aim to estimate the rate $r_{i,1}$ for the first transmission of packet i given the “dispersion” (or interarrival) Δ_i between the two packets at the receiver S . Of course this is possible only when neither of these two packets is lost (at layer-3). Further, we require that packet i is *not* a “tiny-probe”.

Let us first assume that packet i was transmitted only once. In the case of 802.11, and under the assumption of no retransmissions for packet i , the dispersion can be written as:

$$\Delta_i = \frac{S_i}{r_{i,1}} + c + \beta_i \quad (4)$$

using the notation of the previous section. To estimate $r_{i,1}$, we first need to subtract from Δ_i the constant latency term c and the variable delay term β_i which captures the waiting time for the channel to become available and a uniformly random backoff period. The sum of these two terms $c + \beta_i$ is estimated using the tiny-probes; recall that their IP-layer size is only 8 bytes and so their transmission latency is small compared to the transmission latency for the rest of the probing packets. On the other hand, the tiny-probes still experience the same constant

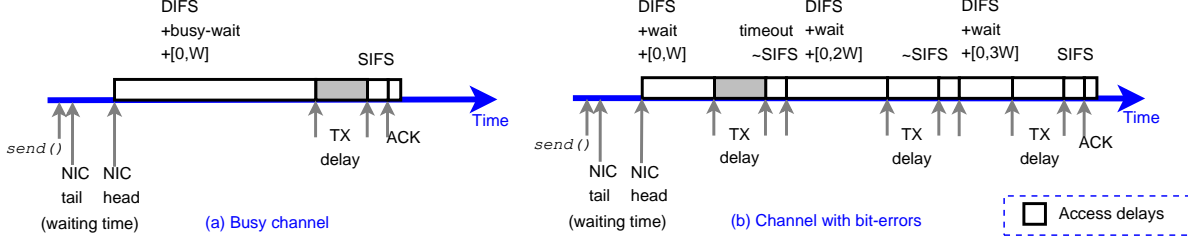


Figure 4: Timeline of an 802.11 packet transmission showing *access delays*.

latency c as larger packets, and their variable-delay β follows the same distribution with that of larger probing packets (because the channel waiting time, or the backoff time, do not depend on the size of the transmitted packet). So, considering only those packet-pairs in which the second packet is a tiny-probe, we measure the *median dispersion* Δ_{tiny} . This median is used as a rough estimate of the sum $c + \beta_i$, when packet i is *not* a tiny-probe.¹ We then estimate the transmission rate $r_{i,1}$ as:

$$r_{i,1} = \frac{s_i}{\Delta_i - \Delta_{\text{tiny}}} \quad (5)$$

If the i 'th packet was retransmitted one or more times, the dispersion Δ_i will be larger than $s_i/r_{i,1} + c + \beta_i$ and the rate will be underestimated. A first check is to examine whether the estimated $r_{i,1}$ is significantly smaller than the lowest possible 802.11 transmission rate (1Mbps). In that case, we reject the estimate $r_{i,1}$ and *flag* that packet. Of course it is possible that some remaining packets have been retransmitted, but without being flagged at this point. We also flag all tiny-probes, as well as any packet i if packet $i - 1$ was lost.

The next step is to map each remaining estimate $r_{i,1}$ to the nearest standardized 802.11 transmission rate $\hat{r}_{i,1}$. For instance, if $r_{i,1} = 10.5\text{Mbps}$, the nearest 802.11 rate is 11Mbps. (note that this transmission rate applies to the 802.11 frame and so s_i has to include the layer-2 headers).

We also exploit the temporal correlations between the transmission rate of successive packets (within the same train) to improve the existing estimates and to produce an estimate for all flagged packets. We have experimented with the four rate adaptation modules available in the MadWiFi driver used with the Atheros chipset (SampleRate, AMRR, Onoe and Minstrel). Figure 5 (top) shows the fraction of probing packets in a train that were transmitted at the most common transmission rate during that train, under three different channel conditions. These results were obtained from 100 experiments with

¹This estimate is revised in the last stage of the algorithm, after we have obtained a first estimate for the transmission rate during a train. We then estimate the transmission latency of each tiny-probe and subtract it from its measured dispersion.

50-packet trains; we also show the Wilcoxon 95% confidence interval in each case. Note that all rate adaptation modules exhibit strong temporal correlations, while three of them (AMRR, Minstrel and Onoe) seem to use a single rate for all packets during a train (each train lasts for 5-250msec, depending on the transmission rate).

Based on the previous strong temporal correlations, we compute the *mode* \tilde{r} (most common value) of the discrete $\hat{r}_{i,1}$ estimates. If the mode includes less than a fraction (30%) of the measurements, we reject that packet train as *too noisy*. Otherwise, we replace every estimate $\hat{r}_{i,1}$, and the estimate for every flagged packet, with \tilde{r} . If most trains show weak modes (i.e., a mode with less than 30% of the measurements), we abort the diagnosis process because the underlying rate adaptation module does not seem to exhibit strong temporal correlations between successive packets. In our experiments, this is sometimes the case with the SampleRate MadWiFi module. In the rest of this work, we only use that rate adaptation module (which is also the default in MadWiFi) because we want to *examine whether the proposed diagnostics work reliably even under considerable rate estimation errors*.

Evaluation: Figure 5 (bottom) shows the accuracy of the proposed rate estimation method under three quite different channel conditions. In particular, we show the *average of the absolute relative error* across all probing packets for which we know the ground-truth transmission rate. The “ground-truth” for each packet was obtained using an AirPcap monitor, positioned close to the sender, that captured most (but not all) probing packets. We detect the first transmission for each packet using the “Retry” flag in the 802.11 header. We see that the inference error is low in most cases; the SampleRate module gives a relatively higher error.

4 Detecting Size-dependent Pathologies

The first “branching point” in the decision tree of Figure 3 is to examine *whether access delays increase with the size of probing packets*. Recall that each probing train consists of packets with eight distinct sizes. The

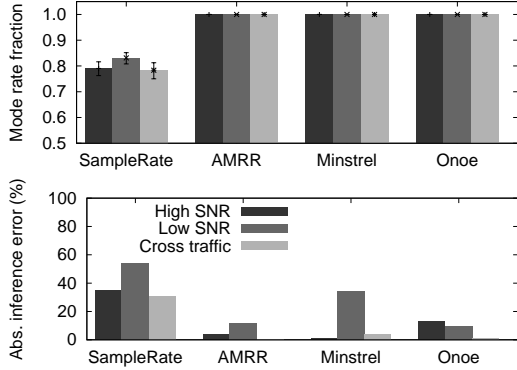


Figure 5: Rate inference: strong temporal correlations between the transmission rate of packets in the same train (top) and rate inference accuracy. Low-SNR conditions are created by separating C and its AP by several meters; congestion is caused by a UDP bulk-transfer over a second network that is in-range.

pathologies in an 802.11 WLAN can be grouped in two categories: a) pathologies that are more likely to increase the access delay of larger packets, because of increased waiting at the sender or increased retransmission likelihood, and b) pathologies that increase the access delay of all packets with the same likelihood, independent of size. We refer to the former as *size-dependent pathologies* and the latter as *size-independent*.

The first category includes a broad class of problems such as bit errors due to noise, fading, interference, low transmission signal strength, or hidden terminals. In the simplest (but unrealistic) case of independent bit errors, the probability that a frame of size s bits will be received with bit errors when the bit-error rate is p is $1 - (1 - p)^s$, which increases sharply with s . Of course, in practice bit errors are not independent and 802.11 frame transmissions are *partially* protected with FEC and rate adaptation techniques. We expect however that when the previously mentioned pathologies are severe enough to cause performance problems, larger packets have a higher probability of being retransmitted, causing an increasing trend between access delay and packet size.

The size-independent class includes pathologies that can also cause large access delays, due to increased waiting at the sender or retransmissions, but where the magnitude of the access delay is independent of the packet size. The best instance in this class is WLAN congestion. It is important, however, that the traffic that causes congestion is generated by WLAN terminals that can “carrier-sense” each other (otherwise we have hidden-terminals). In the case of congestion, the access delays will be larger than the case when there is no congestion (packets have to wait more for the channel to become

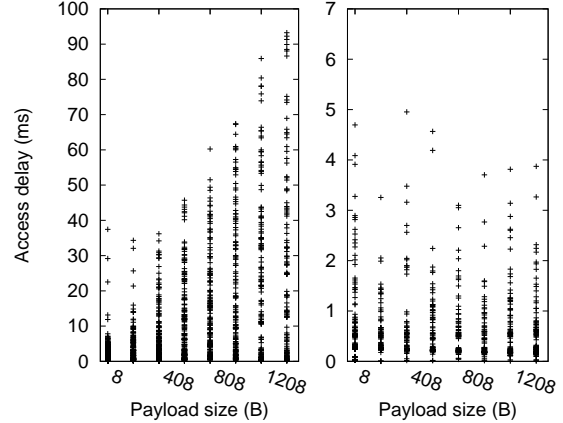


Figure 6: Low signal strength and congestion: effect of packet size (SampleRate module).

available) but the access delays would not depend on the packet size.

Approach: We distinguish between the two pathology classes using statistical trend detection in the relation between access delay and packet size. Figure 6 shows the inferred access delays from experiments with 100 packet trains. In the first experiment (left), the client C and the AP are separated by a large distance of 5-6m, so that C ’s bulk-transfer throughput drops to about 1Mbps. In the second experiment, we attempt to saturate the WLAN with UDP traffic that originates from another terminal. All terminals and APs can carrier-sense each other (we test this based on throughput comparisons when one or more nodes are active). We use 802.11g channel-6 and SampleRate in both experiments.

The access delays in the case of low signal strength increase with the packet size, while this is not true in the case of congestion. A more thorough analysis of these measurements reveals that *not all* access delays increase with the packet size, under low signal strength. Instead, *the increasing trend is clearly observed among those packets that have the larger access delays for each probing size*. This is not surprising: the packets with the larger access delays among the set of packets of a certain size, are typically those that are retransmitted, and the retransmission probability increases with the packet size under size-dependent pathologies. For this reason, instead of examining the average or the median access delay for each packet size, we consider instead the 95-th percentile $\tilde{a}_{95p}(s)$ of the access delays for each packet size s .

The trend detection is performed using the nonparametric Kendall one-sided hypothesis test [12]. The null hypothesis is that there is no trend in the bivariate sample $\{s, \tilde{a}_{95p}(s)\}$ for $s = \{8 + k \times 200, k = 1 \dots 7\}$ (bytes), while the alternate hypothesis is that there is an increas-

ing trend.

Evaluation: For the experiments of Figure 6 the test strongly rejects the null hypothesis under low signal strength with a p-value of 0 (the p-value is less than 0.01 across all MadWiFi rate modules), while the p-value in the case of congestion is 0.81 (0.7-1.0 across all MadWiFi rate modules). We have repeated similar experiments with all other MadWiFi rate adaptation modules and under different signal strengths and congestion levels. The p-values in all experiments show a clear difference between size-dependent and size-independent pathologies, as long as the received signal strength is less than about 8-10dBm. For higher signal strengths, the user-level throughput is more than 5Mbps, and so it is questionable whether there is a pathology that needs to be diagnosed in the first place.

5 Low SNR and Hidden Terminals

After the detection of a size-dependent pathology, WLAN-probe attempts to distinguish between *low-SNR conditions* and *Symmetric Hidden Terminals (SHTs)*. The former represents a wide range of problems (low signal strength, interference from non-802.11 devices, significant fading, and others) - a common characteristic is that they are all caused by *exogenous factors* that affect the wireless channel independent of the presence of traffic in the channel. SHTs represent the case that at least two 802.11 senders (from the same or different WLANs) can not carrier-sense each other and when they both transmit at the same time neither sender's traffic is correctly received. SHTs do not represent an exogenous pathology because the problem disappears if all but one of the colliding senders backoff. The case of asymmetric HTs (or one-node HTs), where one sender's transmissions are corrupted while the conflicting sender's transmissions are correctly received, is no different than the exogenous factors we consider and WLAN-probe will diagnose them as low-SNR.

Approach: To distinguish between low-SNR and SHTs, we first introduce some additional terminology of events that probing packets may see. A probing packet may be *lost at layer-3* (denoted by L3), after a number of unsuccessful retransmissions at layer-2. A probing packet may see an *outlier delay* (OD), if its access delay is significantly higher than the typical access delay in that probing experiment - we classify a packet as OD if its access delay is larger than the sample median plus three standard deviations (the sample includes all measured access delays in that probing experiment - across all trains). Finally, a probing packet may see a *large delay* (LD) if its access delay is higher than the *typical* access delay in that probing experiment - we classify a packet as LD if its access delay is higher than the 90-th

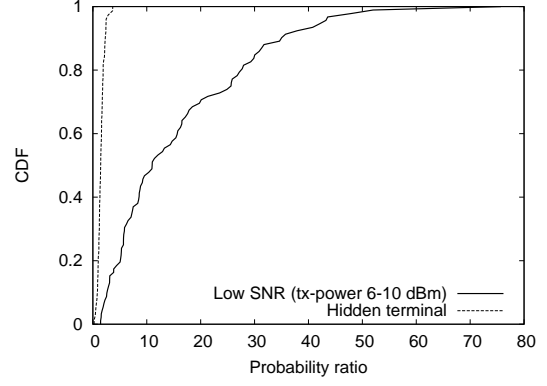


Figure 7: Probability ratio (p_c/p_u) to distinguish between low-SNR and SHT conditions.

percentile of the empirical distribution of access delays (after we have excluded OD packets). Note that the access delays of OD packets are typically much larger than the access delays of LD packets.

The probing and diagnosis process works as follows. The probing packets in this WLAN-probe experiment are of the largest possible size that will not be fragmented. The reason is that larger packets are more likely to collide with other transmissions in the case of SHTs. We then identify all OD or L3 packets in the probing trains of the experiment, and estimate the unconditional probability p_u that either event takes place:

$$p_u = \text{Prob}[\text{OD} \vee \text{L3}] \quad (6)$$

We then focus on the *successor* of an OD or L3 event, i.e., the probing packet that follows an OD or L3 packet. Under low-SNR scenarios we expect that the channel conditions exhibit strong temporal correlations, and so if a packet i experiences an OD or L3 event, its successor packet $i+1$ (denote by *successor*(i)) will see a large delay (LD) or layer-3 loss (L3) event with high probability.

On the other hand, if packet i experiences an outlier delay (OD) or L3 event due to an SHT, the colliding senders will backoff for a random time period and it is less likely that the successor packet will be LD or L3. To capture the previous temporal correlations between an L3 or OD packet and its successor, we consider the conditional probability:

$$p_c = \text{Prob}[\text{successor}(i) : \text{LD} \vee \text{L3} \mid i : \text{OD} \vee \text{L3}] \quad (7)$$

The detection method focuses on the ratio p_c/p_u of the previous conditional and unconditional probabilities. If there is a strong temporal correlation between a probing packet that experiences an OD or L3 event and its successor, this probability ratio will be much larger than one. We expect this to be the case under low-SNR conditions. Otherwise, under an SHTs condition, the previous

temporal correlation is much weaker and the probability ratio will be closer to one.

Evaluation: Figure 7 shows the distribution of the probability ratio p_c/p_u for 100 low-SNR and 90 SHT experiments in our testbed. We create low-SNR conditions by reducing the transmission power of the WLAN-probe client C to 6-10dBm; the access point is about 3m away. We create SHTs conditions using two different networks on 802.11g channel-6, such that the two senders can not carrier-sense each other. When only one sender is active, the throughput in the corresponding network is higher than 10Mbps - when both senders are always backlogged, the throughput drops to less than 1Mbps. The probability ratio is always less than 5 under SHTs, while it is higher than 5 in 80% of the experiments under low-SNR conditions. A probability ratio threshold between 3-5 should be sufficient to diagnose almost all SHTs accurately. Under low-SNR conditions, however, we should expect some diagnosis errors: in 10-20% of the cases, WLAN-probe will diagnose a low-SNR condition as SHT. We are investigating ways to further improve the accuracy of this diagnostic process.

6 Conclusions and future work

We proposed a home WLAN diagnosis process that only requires user-level active probing, and presented some preliminary but promising results that show the feasibility of such diagnostics. A design consideration for our methods is *usability*: we do not require administrative privileges, any form of support from the wireless card/driver/AP, or sensor nodes at vantage points in the home.

We are working on several extensions of WLAN-Probe. First, it is possible that there is no real WLAN pathology - we are working on a method that can distinguish between normal operation and the previous pathologies. Second, some preliminary work shows that we can detect certain non-802.11 interference sources, such as microwave ovens. Third, we are working on improvements in the rate inference method and on testing these methods with additional rate adaptation mechanisms. Finally, we will conduct a larger-scale evaluation of the WLAN-probe diagnostic accuracy with more testbed experiments as well as with actual home WLAN deployments.

References

- [1] WRAPI: API for Real-time Monitoring and Control of an 802.11 Wireless LAN. <http://sysnet.ucsd.edu/pawn/wrapi>, 2002.
- [2] AirMagnet WiFi Analyzer. <http://www.airmagnet.com>, 2010.
- [3] Aruba Networks: RFProtect Spectrum Analyzer. <http://www.arubanetworks.com>, 2010.
- [4] B. Aggarwal, R. Bhagwan, T. Das, S. Eswaran, V.N. Padmanabhan, and G.M. Voelker. NetPrints: Diagnosing home network misconfigurations using shared knowledge. In *USENIX NSDI*, 2009.
- [5] N. Ahmed, U. Ismail, S. Keshav, and K. Papagiannaki. Online estimation of RF interference. In *ACM CoNEXT*, 2008.
- [6] K. Cai, M. Blackstock, M.J. Feeley, and C. Krasic. Non-intrusive, dynamic interference detection for 802.11 networks. In *ACM SIGCOMM IMC*, 2009.
- [7] R. Chandra, V.N. Padmanabhan, and M. Zhang. WiFiProfiler: cooperative diagnosis in wireless LANs. In *ACM Mobisys*, 2006.
- [8] Y.C. Cheng, M. Afanasyev, P. Verkaik, P. Benko, J. Chiang, A.C. Snoeren, S. Savage, and G.M. Voelker. Automating cross-layer diagnosis of enterprise wireless networks. *ACM SIGCOMM CCR*, 37(4):25–36, 2007.
- [9] Y.C. Cheng, J. Bellardo, P. Benko, A.C. Snoeren, G.M. Voelker, and S. Savage. Jigsaw: Solving the puzzle of enterprise 802.11 analysis. *ACM SIGCOMM CCR*, 36(4):39–50, 2006.
- [10] C. Dovrolis, P. Ramanathan, and D. Moore. Packet-dispersion techniques and a capacity-estimation methodology. *Networking, IEEE/ACM Transactions on*, 12(6):963–977, 2004.
- [11] D. Giustiniano, D. Malone, D.J. Leith, and K. Papagiannaki. Measuring transmission opportunities in 802.11 links. *IEEE/ACM ToN*, (99):1, 2010.
- [12] M. Hollander and D.A. Wolfe. *Nonparametric Statistical Methods*. 1999.
- [13] R. Kapoor, L.J. Chen, L. Lao, M. Gerla, and M.Y. Sanadidi. CapProbe: a simple and accurate capacity estimation technique. In *ACM SIGCOMM*, 2004.
- [14] A. Kashyap, S. Ganguly, and S.R. Das. A measurement-based approach to modeling link capacity in 802.11-based wireless networks. In *ACM MOBICOM*, 2007.
- [15] K. Lakshminarayanan, S. Sapra, S. Seshan, and P. Steenkiste. RFDump: an architecture for monitoring the wireless ether. In *ACM CoNEXT*, 2009.

- [16] J. Lee, S.J. Lee, W. Kim, D. Jo, T. Kwon, and Y. Choi. RSS-based carrier sensing and interference estimation in 802.11 wireless networks. In *IEEE SECON*, 2007.
- [17] R. Mahajan, M. Rodrig, D. Wetherall, and J. Zahorjan. Analyzing the MAC-level behavior of wireless networks in the wild. *ACM SIGCOMM CCR*, 36(4):75–86, 2006.
- [18] D. Niculescu. Interference map for 802.11 networks. In *ACM SIGCOMM IMC*, 2007.
- [19] J. Padhye, S. Agarwal, V.N. Padmanabhan, L. Qiu, A. Rao, and B. Zill. Estimation of link interference in static multi-hop wireless networks. In *ACM SIGCOMM IMC*, 2005.
- [20] Marc Portoles-Comeras, Albert Cabellos-Aparicio, Josep Mangués-Bafalluy, Albert Banchs, and Jordi Domingo-Pascual. Impact of transient csma/ca access delays on active bandwidth measurements. In *ACM SIGCOMM IMC*, 2009.
- [21] L. Qiu, Y. Zhang, F. Wang, M.K. Han, and R. Mahajan. A general model of wireless interference. In *ACM MOBICOM*, 2007.
- [22] Charles Reis, Ratul Mahajan, Maya Rodrig, David Wetherall, and John Zahorjan. Measurement-based models of delivery and interference in static wireless networks. *ACM SIGCOMM*, 2006.
- [23] A. Sheth, C. Doerr, D. Grunwald, R. Han, and D. Sicker. MOJO: A distributed physical layer anomaly detection system for 802.11 WLANs. In *ACM Mobisys*, 2006.
- [24] M. Vutukuru, K. Jamieson, and H. Balakrishnan. Harnessing exposed terminals in wireless networks. In *USENIX NSDI*, 2008.